Optimizing Control for Rotor Vibration with Magnetorheological Fluid Damper

Xing Jian (邢健), *He Lidong* (何立东)*, *Wang Kai* (王锎)

Engineering Research Center of Chemical Technology Safety Ministry of Education, Beijing University of Chemical Technology, Beijing, 100029, P. R. China

(Received 25 November 2013; revised 8 March 2014; accepted 22 March 2014)

Abstract: The aim of this work is to analyze and design a control system for vibration reduction in a rotor system using a shear mode magnetorheological fluid (MRF) damper. A dynamic model of the MRF damper-rotor system was built and simulated in Matlab/Simulink to analyze the rotor vibration characteristics and the vibration reduction effect of the MRF damper. Based on the numerical simulation analysis, an optimizing control strategy using pattern search method was proposed and designed. The control system was constructed on a test rotor bench and experiment validations on the effectiveness of the proposed control strategy were conducted. Experimental results show that rotor vibration caused by unbalance can be well controlled whether in resonance region (70%) or in non-resonance region (30%). An irregular vibration amplitude jump can be suppressed with the optimization strategy. Furthermore, it is found that the rapidity of transient response and efficiency of optimizing technique depend on the pattern search step. The presented strategies and control system can be extended to multi-span (more than two or three spans) rotor system. It provides a powerful technical support for the extension and application in target and control for shafting vibration.

Key words: magnetorheological fluid damper; optimizing control; pattern search method; vibration reduction

CLC number: TP273.1 **Document code**: A **Article ID**: 1005-1120(2014)05-0538-08

1 Introduction

Rotating machines represent the largest and most important class of machinery including aircraft gas turbine engine, electrical motors, machine tools, compressors and turbo machinery. These systems are affected by exogenous or endogenous vibrations produced by unbalance, misalignment and cracks, etc. Reduction of rotor vibration is very important for safe and efficient functioning of these rotating machines. Applying damping to rotor supports is a popular technique for vibration reduction. Among other damping devices (active magnetic bearing[1], squeeze film damper and electrorheological damper), magnetorheological fluid (MRF) damper, which provides adjustable damping over a wide range of frequencies without large power requirements[2], is one of the more promising new devices. It has been successfully used in civil engineering and other engineering applications. Ni, et al.[3] used semi-active MRF dampers for cable vibration control of the bridge under wind rain excited conditions. Fujitani[4] developed a 400 kN MRF damper for a real base-isolated building. The Bose suspension system is a typical and successful technical realization in automotive suspension. Francesc Pozo[5] applied the semi-active vehicle stability control for vibration reduction. Various control techniques have been proposed to improve the performance of vibration reduction. Karimi[6] applied an optimal control technique for vehicle engine body system using Haar functions. Adaptive fuzzy neural network control technique designed

Foundation items: Supported by the National Program on Key Basic Research Program ("973" Program) (2012CB026000); the Ph. D. Programs Foundation of Ministry of Education of China (20110010110009).

* **Corresponding author**: He Lidong, Professor, E-mail: he63@263.net.

by Yu, et al.[7] for magnetorheological suspension. Wang, et al.[8] designed an active landing gear system to reduce aircraft vibrations with proportion-integration-differentiation (PID) strategy.

There are two kinds of MRF dampers used in rotor vibration, i. e., the MRF squeeze film damper (MRFSFD) and the shear mode MRF damper. Wang and Meng[9] designed a single disk rotor system supported on a squeeze MRF damper referring to the rotor and supporting the structure of small aero-engines. Compared with the MRFSFD which has the disadvantages of high instability, limited inhibition of critical vibration and delayed responses, the shear mode MRF damper achieves better vibration suppression with the quicker responses. Research literatures related to shear mode MRF damper in rotor vibration reduction mainly focus on simple control technique (on-off method). Rotor vibration is well controlled in resonance region with an on-off control technique[10]. Furthermore, the increasing of current leads to a considerable decrease of rotor vibration amplitude. However, the rising current may also cause instability to rotor system. Improper current may cause rotor system losing stability. It is thus necessary to apply the current properly to MRF damper to get better performance. Due to the complex dynamic behavior of the rotor system and the MRF damper, few literatures till now have focused on the optimizing control for the rotor vibration using shear mode MRF damper. For this, a shear mode MRF damper and a vibration active control system were designed in this paper. An optimizing control scheme was presented to reduce vibration dynamically on line with the optimal current.

2 MRF Damper-Rotor System Modeling and Numerical Analysis

2.1 MRF damper modeling and analysis

Geometry of the designed shear mode MRF damper is illustrated in Fig. 1. It has three moving disks and two stationary disks. The disks are

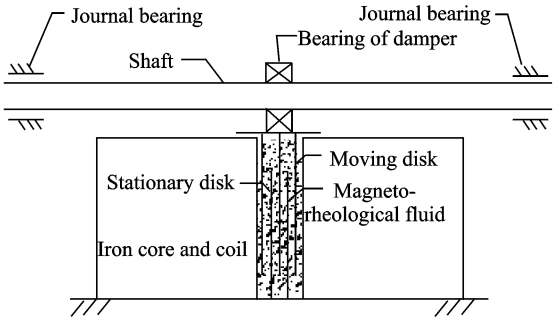

Fig. 1 Geometry of the shear mode MRF damper

placed uniformly and alternatively with a uniform gap of 1 mm to form six relative shear surfaces. Electric current is input to the coil to generate magnetic field. The MRF in the MRF damper can be described by the Bingham plastic model. The Bingham plasticity model is effective in describing the essential field-dependent fluid characteristic. It can be described in the stress-strain relationship as follows[11]

$$\tau = \tau_y(H)\,\mathrm{sgn}(\dot{\gamma}) + \eta\dot{\gamma} \tag{1}$$

where τ is the fluid shear stress, τ_y the yield stress variable to magnetic field strength H, η the MR fluid viscosity when no magnetic field applied, $\dot{\gamma}$ the shear-strain rate, and $\mathrm{sgn}(\dot{\gamma})$ the signum function for shear-strain rate. The relationship of τ_y and H holds[12]

$$\tau_y = 2.769\,0\times10^{-6}\times H^3 - 0.002\,3\times H^2 + 0.636\,7\times H - 5.119\,8 \tag{2}$$

The damper force is obtained by the integral of τ on the whole shear surface[13]

$$F_{MR} = F_\eta + F_\tau \tag{3}$$

where F_{MR} is the damper force, F_τ the controllable force due to the controllable yield stress τ, and F_η the viscous force, which can be computed by

$$F_\eta = C_{eq}\cdot v_{MR}(t) \tag{4}$$

$$F_\tau = n_{sr}\cdot s_{sr}\cdot \tau_y \tag{5}$$

$$C_{eq} = C_0 + C_{MR}\cdot i \tag{6}$$

$$C_{MR} = \frac{n_{sr}\cdot s_{sr}\cdot \eta}{w} \tag{7}$$

$$\dot{\gamma} = \frac{v_{MR}(t)}{w} \tag{8}$$

where $v_{MR}(t)$ is the move speed of the MRF damper ball bearing center, w the width of the

gap between parallel plates (moving disk and stationary disk), n_{sr} the number of shear disk, S_{sr} the effective shear area, η the Newtonian viscosity, and C_{eq} the equivalent damping coefficient of MRF damper (related to controlled current i).

2.2 MRF damper-rotor system modeling and analysis

The analyzed rotor consists of a shaft and one disk supported by journal bearings at both its ends. A designed MRF damper is mounted on the rotor shaft. Fig. 2 is the simplified mechanical model of MRF damper-rotor system.

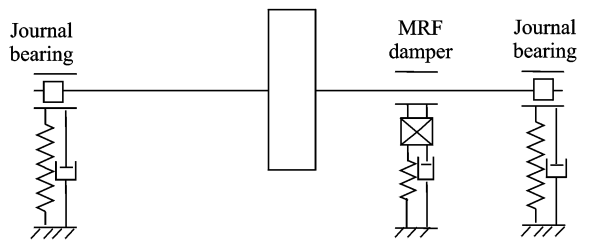

Fig. 2 Mechanical model of MRF damper-rotor system

According to the Lagrange equation of the non-conservative system[14]

$$\frac{\mathrm{d}}{\mathrm{d}t}\left(\frac{\partial L}{\partial \dot{q}_i}\right)-\frac{\partial L}{\partial q_i}+\frac{\partial \Phi}{\partial \dot{q}_i}=Q_i \qquad i=1,2,\cdots,n \tag{9}$$

where L is the Lagrange function, Φ the dissipation energy of the system. Q_i and q_i are the generalized coordinates and forces of the system, respectively. The dynamics equation of rotor-MRF damper can be expressed as

$$\begin{cases} \boldsymbol{M}\ddot{\boldsymbol{X}}+\boldsymbol{C}\dot{\boldsymbol{X}}+\boldsymbol{K}\boldsymbol{X}=\boldsymbol{F}_x(t)+\boldsymbol{F}_{\mathrm{MR}x}(t) \\ \boldsymbol{M}\ddot{\boldsymbol{Y}}+\boldsymbol{C}\dot{\boldsymbol{Y}}+\boldsymbol{K}\boldsymbol{Y}=\boldsymbol{F}_y(t)+\boldsymbol{F}_{\mathrm{MR}y}(t) \end{cases} \tag{10}$$

where $\boldsymbol{M}$ is the mass matrix, $\boldsymbol{C}$ the damping matrix, $\boldsymbol{K}$ the stiffness matrix, $\boldsymbol{F}(t)$ the force matrix including journal bearing force and unbalance force, and $\boldsymbol{F}_{\mathrm{MR}}(t)$ the damping force matrix. According to Eqs. (1—8)

$$\begin{cases} \boldsymbol{F}_{\mathrm{MR}x}=\boldsymbol{F}_\tau\cos\theta+\boldsymbol{F}_{\eta x}=\boldsymbol{F}_\tau\cos\theta+C_{\mathrm{eq}}\dot{\boldsymbol{X}}_{\mathrm{MR}} \\ \boldsymbol{F}_{\mathrm{MR}y}=\boldsymbol{F}_\tau\sin\theta+\boldsymbol{F}_{\eta y}=\boldsymbol{F}_\tau\sin\theta+C_{\mathrm{eq}}\dot{\boldsymbol{Y}}_{\mathrm{MR}} \end{cases} \tag{11}$$

where θ is the angle between $v_{\mathrm{MR}}(t)$ and the x axis. The dynamic equation of MRF damper-rotor system is

$$\begin{cases} \boldsymbol{M}\ddot{\boldsymbol{X}}+\boldsymbol{C}(i)\dot{\boldsymbol{X}}+\boldsymbol{K}(i)\boldsymbol{X}=\boldsymbol{F}_x+\boldsymbol{f}_x(i) \\ \boldsymbol{M}\ddot{\boldsymbol{Y}}+\boldsymbol{C}(i)\dot{\boldsymbol{Y}}+\boldsymbol{K}(i)\boldsymbol{Y}=\boldsymbol{F}_y+\boldsymbol{f}_y(i) \end{cases} \tag{12}$$

The basic structure parameters of the rotor system are shown in Table 1. Assume that an unbalance value (0.15 kg · mm) was put on the disk (the zero phase) to analyze the unbalanced synchronous response of the rotor system. The MRF damper-rotor system was simulated with Matlab/Simulink. During simulation, an unbalanced force was applied and the Runge-Kutta equations of the system model were adopted during calculation.

Table 1 Basic parameters of the rotor system

Parameter	Value
Density /(kg · m^{-3})	7 980
Modulus of elasticity/GPa	210
Mass of rotor/g	506
Diameter of rotor/mm	75
Width of rotor/mm	15
Diameter moment of inertia of the rotor/(kg · m^2)	0.000 176
Polar moment of inertia of the rotor/(kg · m^2)	0.000 352
Length of the working shaft/mm	505
Working shaft span/mm	470
Diameter of shaft/mm	10

The frequency response characteristics of the rotor system with three different work conditions (without damper, small current and large current) are depicted in Fig. 3.

It indicates that rotor vibration is well controlled in resonance region with the shear mode MRF damper. Furthermore, the increasing of current leads to a considerable decrease of rotor

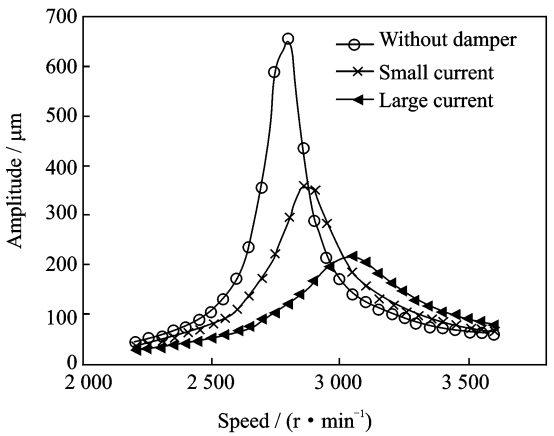

Fig. 3 Comparison of rotor with and without damper

vibration amplitude. However, the rising current increases the first critical speed of the rotor system and may also cause instability to rotor system. Since MRF damper will largely increase the support stiffness, it may cause the stability lost of the rotor system. It is thus necessary to control the current properly for better performance.

3 Design of Optimizing Control Strategy Using Pattern Search Methods

Based on the modeling and numerical analysis, an optimizing control strategy using pattern search method, which is a subset of direct search algorithm introduced by Hooke, et al.[15], was proposed and designed.

It needs to confirm a search pattern $\boldsymbol{P}_k$ and an exploratory move s_k. The pattern matrix $\boldsymbol{P}_k$ is specified as follows

$$\boldsymbol{P}_k = \boldsymbol{B} \times \boldsymbol{C}_k \tag{13}$$

where $\boldsymbol{B} \in \mathbf{R}^{n \times n}$ is a basis matrix fixed in every iteration, $\boldsymbol{C}_k$ a generating matrix that can vary from iteration to iteration. The description of the pattern was introduced in the unconstrained case in order to unify the features of such disparate algorithms as the method of Hooke, et al.[15]

The matrix $\boldsymbol{B}$ will be ignored ($\boldsymbol{B}=\boldsymbol{I}$) in linearly constrained problems. After the search pattern settled, pattern search methods proceeds by a series of exploratory moves about the current iterate x_k to choose a new iterate x_{k+1}.

In the analysis of pattern search methods

$$\boldsymbol{P}_k = \boldsymbol{C}_k = [c_k^1 \cdots c_k^{pk}] = [\boldsymbol{\Gamma}_k \quad \boldsymbol{L}_k] \tag{14}$$

For the step $\Delta_k \in \mathbf{R}$, $\Delta_k > 0$, assume exploratory move $s_k^i = \Delta_k c_k^i$

$$s_k \in \Delta_k \boldsymbol{P}_k \equiv \Delta_k [\boldsymbol{\Gamma}_k \quad \boldsymbol{L}_k] \tag{15}$$

If $\min\{f(x_k + y) \mid y \in \Delta_k \boldsymbol{\Gamma}_k \text{ and } (x_k + y) \in \Omega\} < f(x_k)$, then

$$f(x_k + s_k) < f(x_k) \tag{16}$$

If Eqs. (15,16) are valid, then

$$x_k + 1 = x_k + s_k$$

where x_k is the current iterate and Ω the feasible region for x. $\boldsymbol{\Gamma}_k \in \mathbf{Z}^{n \times rk}$ belongs to a finite set of matrices Γ with certain geometrical properties. $\boldsymbol{L}_k \in \mathbf{Z}^{n \times (pk-rk)}$ contains at least a column of zeros, which means a zero step. R, Q and N are the sets of real, rational and natural numbers, respectively.

Pattern search methods explore the design space in a more restrictive manner. The moves are allowed only along the pattern directions. The step sizes are updated according to certain rules, with large steps used early in the search and scaled down gradually during the search.

To design an optimizing controller using pattern search methods for rotor vibration reduction, we must specify the pattern $\boldsymbol{P}_k$, the exploratory moves to be used to produce a feasible step s_k and the algorithms for updating $\boldsymbol{P}_k$ and Δ_k. The control principle scheme of the optimization seeking strategy is shown in Fig. 4.

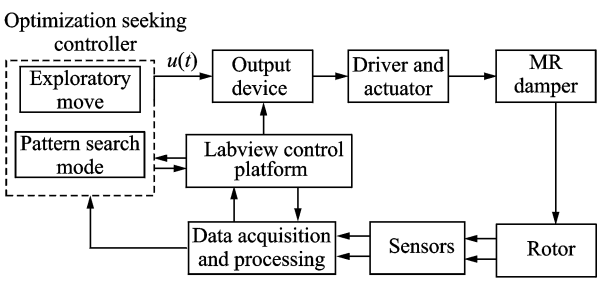

Fig. 4 Control scheme of optimization seeking strategy

The controller is designed and accomplished in the Labview platform. The search program flow chart is illustrated in Fig. 5.

An initial control current state $u_0 \in \Omega$ is chosen and the step Δ_0 be given by simulation. The objective function for that state is evaluated and determined by simulation. The evaluating function $f(u_k)$ is computed (for $k=0,1,\cdots$), and a step s_k is determined using a linearly constrained exploratory moves algorithm. If $f(u_k + s_k) < f(u_k)$, then $u_{k+1} = u_k + s_k$; otherwise, $u_{k+1} = u_k$, update P_k and Δ_k. The search continues from the current state along the next pattern direction, following the same criteria of the new state acceptance. The search stops when the objective function meets the desired value. To simplify the control program, a fixed search step is chosen in this paper.

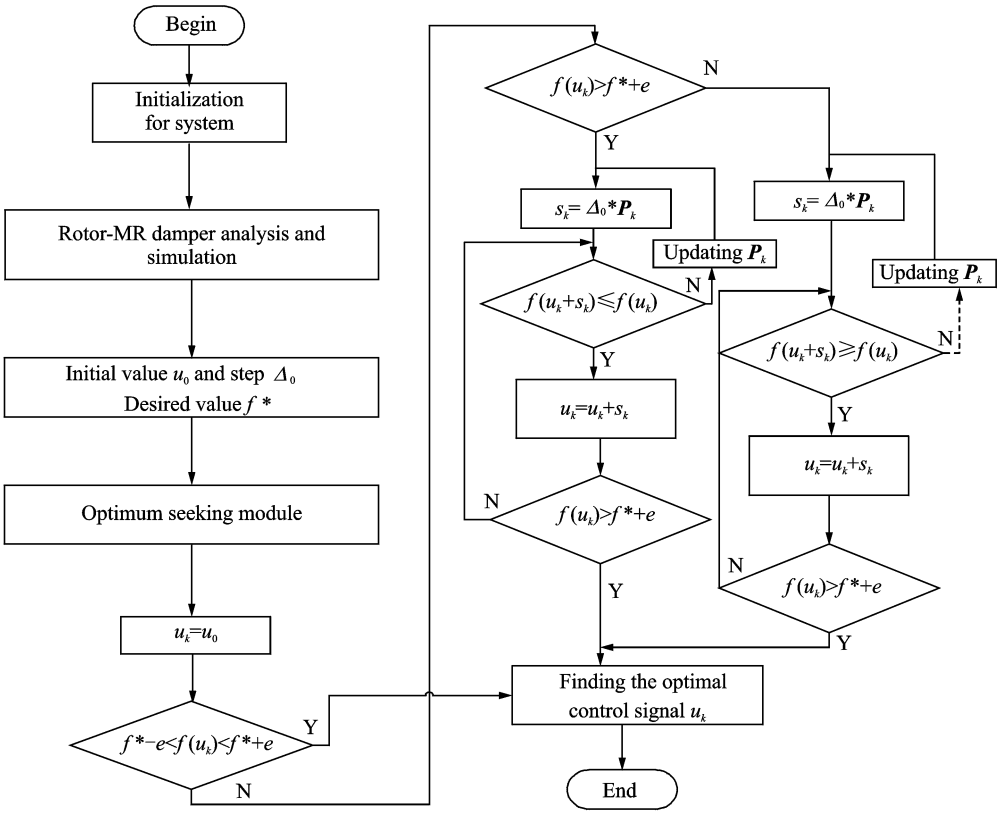

Fig. 5 Flow chart of optimization seeking algorithm

4 Experimental Validations and Result Analyses

In order to experimentally validate and evaluate the control performance, a control system was designed and constructed, the schematic diagram of the experiment system and the sketch of the rotor system with MRF damper are shown in Fig. 6.

The rotor system was outfitted with eddy-current type non-contact displacement sensor that measures the displacements of the flexible rotor. A real-time control and data acquisition system was designed to collect the vibration data and regulate the input current to the MRF damper.

Based on the simulation and experiments, an initial current for MRF damper and seeking step Δ_0 were determined. The control program was implemented according to the flow chart in Fig. 5. Experiments were arranged and conducted under

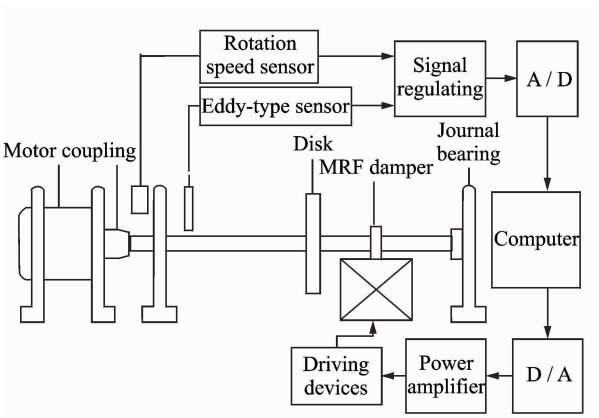

(a) Control principle of MRF damper-rotor system

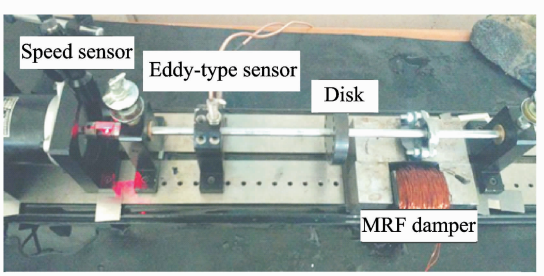

(b) Rotor bench with MRF damper

Fig. 6 Principle and components of the MRF damper-rotor system

]two different work conditions. The effectiveness of optimizating control strategy for rotor vibration was studied in rotor run-up process and at rotor vibration amplitude jump.

4.1 Vibration suppression in the rotor run-up process with different desired vibration amplitudes

When the rotor was accelerating, according to the optimization seeking strategy, an appropriate current was searched and applied. Current optimization seeking process with different desired values (140, 180 and 220 μm) are illustrated in Fig. 7.

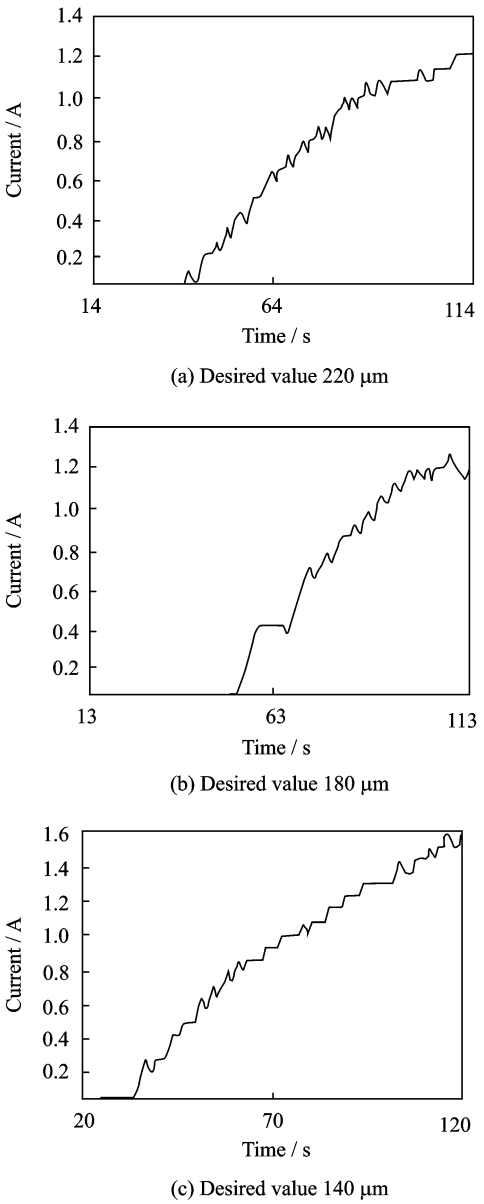

Fig. 7 Current optimization seeking process with three different desired values

The frequency response of rotor system using MRF damper with different desired values and original rotor vibration is illustrated in Fig. 8.

Note that the experimental results (Figs. 7, 8) show the seeking processes of currents and the effectiveness of the control strategy. With three different desired control target values, the control strategy is effective in the vibration suppression, and the current varying with the rotor vibration to find an appropriated current. The rotor vibration has been decreased by 70% in resonance region and 30% in non-resonance region, which implies that rotor vibration caused by unbalance is well controlled whether in the resonance or non-resonance regions with optimization seeking strategy. With the current applied appropriately, it will not lead to instability of the rotor system.

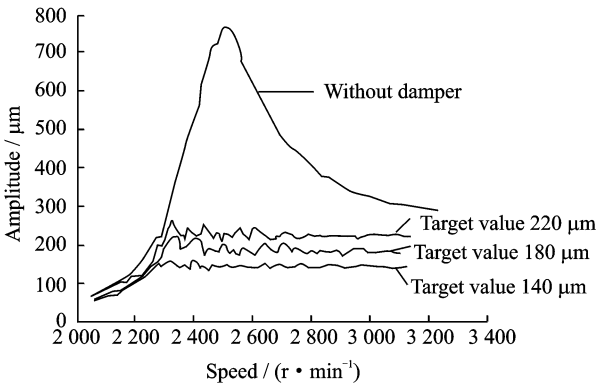

Fig. 8 Comparison of rotor vibration with damper (three target values) and without damper

4.2 Vibration suppression when rotor vibration jump occurs

The rotor was running stably at certain speed and amplitude. When vibration amplitude suddenly changed, an optimal current searched by the optimizing control strategy was applied on the rotor system to control the rotor vibration in the target value (140 μm). Experiments were conducted in two different search steps (0.05 and 0.1 A) to evaluate the efficiency and effectiveness of the control strategy.

The amplitude and current responses curves are shown in Fig. 9. The vibration amplitude jumps regulated by hand, in which rising jumps occur at lines ab and a^*b^*, and descending jump

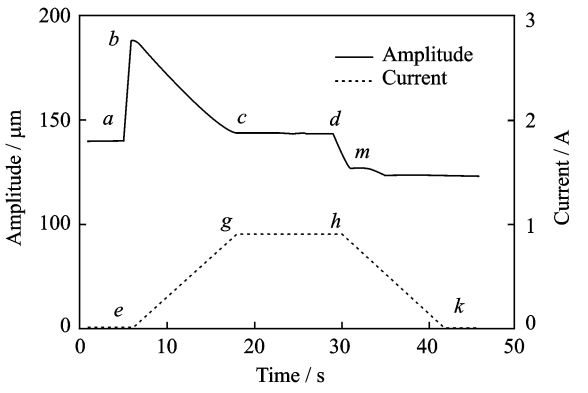

(a) Amplitude and current response with search step 0.05 A

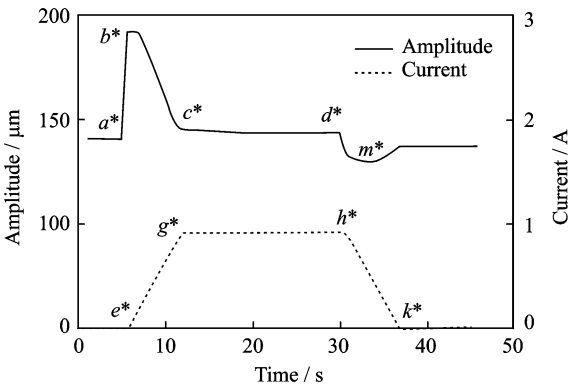

(b) Amplitude and current response with search step 0.1 A

Fig. 9 Amplitude and current response with optimization seeking strategy

occur at dm and d^*m^*. The vibration amplitude jump can be suppressed by two search steps. Compared the curve descending between Fig. 9(a) (from point b to c) and Fig. 9(b) (from point b^* to c^*), the smaller the search step, the flatter the descending portion of the curve, the longer searching time for appropriated control currents (seen curve rising at line eg and e^*g^*, curve descending at line hk and h^*k^*), and the lower response of the vibration suppression, but more smooth than that of larger search step. With a larger search step, the transient response is more rapid but less steady than that with smaller search step.

5 Conclusions

(1) According to the on-line monitoring for vibration amplitude, the current can be adjusted in real-time to achieve on-line dynamic vibration control during a rotor run-up process. It indicates that rotor vibration caused by unbalance is well controlled in both resonance and non-resonance regions with the appropriate current control which prevents the rotor system from instability. It provides a powerful technical support for the extension and application in aerospace engineering or other rotating machinery.

(2) When the rotor is running stably at certain speed and amplitude, a sudden jump in rotor vibration amplitude should be avoided, which can be suppressed by the optimizing control strategy using pattern direct search algorithms effectively and quickly.

(3) The rapidity of transient response and efficiency of optimization seeking technique for rotor system depend on the pattern search step. A fixed search step is used in this paper. Further research on search step varying with different vibration amplitude can be peformed to improve the efficiency smoothness and rapidity of transient vibration response.

The strategies and control system presented in this paper can be extended to multi-span (more than two or three spans) rotor system. It can also be applied to other vibration control techniques, for instance, anti-swirl, which provides a powerful technical support for the extension and application in target and control for shafting vibration.

References:

[1] Gao Hui, Xu Longxiang, Zhu Yili. Compensation control of real-time unbalance force for active magnetic bearing system[J]. Transactions of Nanjing University of Aeronautics and Astronautics, 2011,28(2):183-191.

[2] Zhang Buyun, Chen Huaihai, He Xudong, et al. Experimental study on damping characteristic of magneto rheological damper[J]. Journal of Nanjing University of Aeronautics & Astronautics, 2012, 44(6): 855-861. (in Chinese)

[3] Ni Y Q, Duan Y F, et al. Damping identification of MR-damped bridge cables from in-site monitoring under wind-rain-excited conditions[C]// Proceedings of SPIE. [S. l.]: The International Society for Optical Engineering, 2002(4696):41-51.

[4] Fujitani H. Development of 400 kN magnetorheolog-

ical damper for a real base-isolated building[C]// Proceedings of SPIE Conference Smart Structures and Materials. Bellingham, England: SPIE-International Society for Optical Engineering, 2003(5052): 265-276.

[5] Francesc Pozo, Mauricio Zapateiro, Leonardo Acho, et al. Experimental study of semi-active VSC techniques for vehicle vibration reduction[J]. Journal of the Franklin Institute, 2013(350): 1-18.

[6] Karimi H R. Optimal vibration control for vehicle engine-body system using Haar functions[J]. International Journal of Control Automation and Systems, 2006,4:714-724.

[7] Yu Miao, Dong Xiaomin, Liao Changrong, et al. Adaptive fuzzy neural network control for magnetorheological suspension[J]. International Journal of Computer Science and Network Security, 2006(6): 66-71.

[8] Wang H, Xing J T, Price W G, et al. An investigation of an active landing gear system to reduce aircraft vibrations caused by landing impacts and runway excitations[J]. Journal of Sound and Vibration, 2008(317):50-66.

[9] Wang J X, Meng G. Experimental study on rotor system vibration control of a squeeze MR fluid damper[J]. Journal of Aerospace Power, 2005,20(3): 424-428. (in Chinese)

[10] Wang J, Meng G. Experimental study on stability of an MR fluid damper-rotor journal bearing system[J]. Journal of Sound and Vibration, 2003(262): 999-1007.

[11] Stanway R, Sposton J L, Stevens N G. Non-linear modeling of an electrorheological vibration damper [J]. J Electrostatics, 1987,20:167-184.

[12] Ningbo ShanGong Center. Magnetorheological fluid [EB/OL]. http://www. nbshangong. com/product-show-en, [2014-03-31].

[13] Liu Y H. The finite element analysis of magneto rheological damper-rotor system [D]. Guangzhou: South China University of Technology, 2011: 24-30. (in Chinese)

[14] Zhong Y E, He Y Z, Wang Z, et al. Rotordynamics [M]. Beijing: Tsinghua University Press, 1987: 8-13. (in Chinese)

[15] Hooke R, Jeeves T A. Direct search solution of numerical and statistical problems[J]. J Assoc Comput Mach, 1961, 8(2): 212-229.

(Executive editor: Zhang Tong)